



## Structural characterization, biological evaluation and DNA interaction of some potential drugs based on bifunctional aldehyde functionality

Mehwish Naz <sup>1</sup>, Zareen Akhter <sup>1,\*</sup>, Ayesha Zaka <sup>2</sup>, Bushra Mirza <sup>2</sup>, Vickie McKee <sup>3</sup>, Ehsan Ullah <sup>2</sup> and Michael Bolte <sup>4</sup>

<sup>1</sup> Department of Chemistry, Quaid-i-Azam University, Islamabad, 45320, Pakistan

<sup>2</sup> Department of Biochemistry, Quaid-i-Azam University, Islamabad, 45320, Pakistan

<sup>3</sup> Department of Chemical Sciences, Dublin City University, Glasnevin, Dublin, 9, Ireland

<sup>4</sup> Institut für Anorganische Chemie, Johann Wolfgang Goethe-Universität, Frankfurt/Main, D-60438, Germany

\* Corresponding author at: Department of Chemistry, Quaid-i-Azam University, Islamabad, 45320, Pakistan.

Tel.: +92.51.90642111. Fax: +92.51.90642241. E-mail address: [zareenakhter@yahoo.com](mailto:zareenakhter@yahoo.com) (Z. Akhter).

### ARTICLE INFORMATION



DOI: 10.5155/eurjchem.8.3.195-202.1576

Received: 21 April 2017

Received in revised form: 29 May 2017

Accepted: 05 June 2017

Published online: 30 September 2017

Printed: 30 September 2017

### KEYWORDS

Hyperchromism

DNA damaging assay

Bifunctional aldehyde

Chemotherapeutic agent

Pharmacological activities

Bifunctional aldehyde-DNA interaction

### ABSTRACT

Recent work aimed at evaluating the possibility of enhancing biological activities by synthetically modifying bifunctional aldehyde structures. In this article, two series of bifunctional aldehydes were synthesized, structurally characterized (M-1A, M-1C and M-2A) using single crystal X-ray diffraction analysis. Several pharmacological properties like cytotoxic, antifungal, antibacterial, antioxidant and antitumor activities were also evaluated. In addition, bifunctional aldehyde-DNA interaction assay was examined by UV-Vis spectroscopy which revealed the DNA damaging behaviour of these aldehydes. The results of UV-Vis spectroscopy were supported by DNA damaging assay. The overall results reveal that bifunctional aldehyde moiety could be used as potential drug candidates.

Cite this: *Eur. J. Chem.* 2017, 8(3), 195-202

### 1. Introduction

Aldehydes are responsive molecules that are involved in biochemical, physiological and pharmacological processes [1,2]. Overall natural existence of unsaturated bifunctional aldehyde also highlights the biological prominence of this functional group and possesses antimicrobial and antifeedant activities [3]. Many of the biologically active have been proposed to be active agents in natural chemical defense systems [4], an enzyme [5], antimicrobial activity [6], disinfectant [7], antifungal activity [8], algacidal and cytotoxic activity [9]. Some of these compounds could stabilize or fix the damaged cell membrane [10].

Bifunctional aldehydes also exist in nature as potent antitumor agents [11]. Aromatic aldehydes and adducts against TLX 5 lymphoma in mice show antitumor activity [12]. A series of aralkyl aldehydes were also tested which indicated positive results against antitumor activity [13]. Aromatic anthracyclines containing the aldehyde moiety also demonstrated antitumor activity [14].

Aldehydes form adducts with DNA, RNA, and proteins induce impaired cellular homeostasis, enzyme inactivation, DNA damage, and cell death [15-17]. Generally, aldehyde interact with DNA bases, either directly by reacting with DNA bases, by spawning more reactive bifunctional intermediates, which lead to the formation of exocyclic DNA adducts or ethenobases which cause DNA damage. Of these, 4-hydroxy-2-nonenal (HNE), malondialdehyde (MDA), acrolein, and crotonaldehyde have been most deeply considered regarding their chemical and biological interactions with nucleic acids [18].

In the present work, we have synthesized and characterized a series of aliphatic and aromatic spacer containing bifunctional aldehydes (4,4'-diformyl- $\alpha,\omega$ -diphenoxybutane (M-1A), 4,4'-diformyl-3,3'-methoxy- $\alpha,\omega$ -diphenoxybutane (M-1B) and 4,4'-diformyl-3,3'-ethoxy- $\alpha,\omega$ -diphenoxybutane (M-1C), 4,4'-diformyl- $\alpha,\omega$ -diphenoxy-*p*-xylene (M-2A), 4,4'-diformyl-3,3'-methoxy- $\alpha,\omega$ -diphenoxy-*p*-xylene (M-2B), 4,4'-diformyl-3,3'-ethoxy- $\alpha,\omega$ -diphenoxy-*p*-xylene (M-2C) to study the pharmacological activities [19].

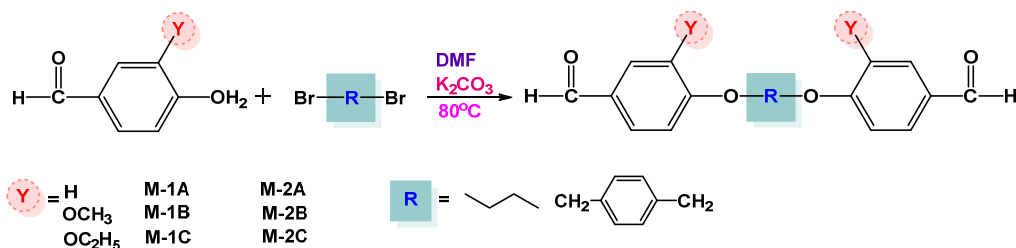


Figure 1. Synthesis of aliphatic and aromatic spacer containing series of bifunctional aldehydes.

In this connection, numerous bioassays and DNA-drug interactional studies are performed. *In vitro* DNA-bifunctional aldehyde interaction of these compounds was evaluated by spectrophotometric technique. DNA damaging studies were also done to confirm the damaging behavior of bifunctional aldehyde.

## 2. Experimental

### 2.1. Materials and methods

4-Hydroxybenzaldehyde, 4-hydroxy-3-methoxybenzaldehyde, 1,4-dibromobutane, 4-hydroxy-3-ethoxybenzaldehyde, 1,4-dibromo-*p*-xylene and solvents were purchased from Sigma Aldrich. Potassium carbonate purchased from Fluka. Melting point was checked on the melting point apparatus model MP-D Mitamura Riken Kogyo (Japan). FT-IR spectra were taken on ThermoScientific NICOLET 6700 FT-IR. Nuclear magnetic resonance was carried out by using Bruker Avance 300 digital NMR in DMSO-*d*<sub>6</sub> as solvent and tetramethylsilane as an internal standard. The solution of commercial Salmon DNA ( $6 \times 10^4$  M) was prepared and its concentration was measured by UV absorbance at 260 nm. Prepared stock solution of DNA was protein free because A260/A280 > 1.8. Rest concentrations of DNA were prepared from the prepared stock solution. UV-Visible studies of dilute bifunctional aldehyde solutions in dried ethanol were performed on Shimadzu, 1998, 2000.

### 2.2. Synthesis of bifunctional aldehyde

Aliphatic and aromatic spacer containing based bifunctional aldehyde were prepared [19,20] by dissolving 4-hydroxybenzaldehyde (0.02 mole),  $\alpha,\omega$ -dibromobutane (M-1A) or 1,4-dibromo-*p*-xylene (M-2A) (0.01 mole) and potassium carbonate (50 mmol) in DMF and stirred for 24 h at 80 °C, the formation of product was monitored by TLC (chloroform: methanol, 90:10, v:v). The reaction mixture was poured in water (200 mL) and the precipitated crystals were filtered out and recrystallized from ethanol and water mixture (50:50, v:v) to get the bifunctional aldehyde as product (Figure 1). Substituted bifunctional aldehyde products were synthesized following the procedure [19,20] described in the above paragraph except that 4-hydroxy-3-methoxybenzaldehyde (M-1B and M-2B) and 4-hydroxy-3-ethoxybenzaldehyde (M-1C and M-2C) were used instead of 4-hydroxybenzaldehyde and the crude product thus obtained.

**4,4'-Diformyl- $\alpha,\omega$ -diphenoxybutane (M-1A):** Yield: 72%. M.p.: 104-106 °C. FT-IR (KBr, v, cm<sup>-1</sup>): 2932 (Aliphatic CH), 1682 (CO), 1596 (C=C), 1510 (C=C), 1230 (C-O-C). <sup>1</sup>H NMR (300 MHz, DMSO-*d*<sub>6</sub>,  $\delta$ , ppm): 2.50 (m, 4H, CH<sub>2</sub>), 4.16 (t, 4H, O-CH<sub>2</sub>, <sup>3</sup>J = 8.7 Hz), 7.16-7.36 (m, 8H, Ar-H), 9.81 (s, 2H, Ar-CHO). <sup>13</sup>C NMR (75 MHz, CDCl<sub>3</sub>,  $\delta$ , ppm): 25.00-29.00 (CH<sub>2</sub>), 68.50 (Ar-O-CH<sub>2</sub>), 115.37-164.06 (Ar-C), 191.76 (CHO).

**4,4'-Diformyl-3,3'-methoxy- $\alpha,\omega$ -diphenoxybutane (M-1B):** Yield: 76%. M.p.: 98-100 °C. FT-IR (KBr, v, cm<sup>-1</sup>): 2928

(Aliphatic CH), 1684 (CO), 1587 (C=C), 1517 (C=C), 1233 (C-O-C). <sup>1</sup>H NMR (300 MHz, DMSO-*d*<sub>6</sub>,  $\delta$ , ppm): 2.69 (m, 4H, CH<sub>2</sub>), 3.60 (t, 4H, O-CH<sub>2</sub>, <sup>3</sup>J = 8.3 Hz), 3.70 (s, 6H, CH<sub>3</sub>-O-Ar), 7.10-7.90 (m, 6H, Ar-H), 9.83 (s, 2H, Ar-CHO). <sup>13</sup>C NMR (75 MHz, CDCl<sub>3</sub>,  $\delta$ , ppm): 64.50 (O-CH<sub>3</sub>), 69.81 (Ar-O-CH<sub>2</sub>), 128.51-136.66 (Ar-C), 191.68 (OHC).

**4,4'-Diformyl-3,3'-ethoxy- $\alpha,\omega$ -diphenoxybutane (M-1C):** Yield: 78%. M.p.: 157-159 °C. FT-IR (KBr, v, cm<sup>-1</sup>): 2927 (Aliphatic CH), 1678 (CO), 1593 (C=C), 1519 (C=C), 1229 (C-O-C). <sup>1</sup>H NMR (300 MHz, DMSO-*d*<sub>6</sub>,  $\delta$ , ppm): 2.70 (m, 6H+4H, CH<sub>3</sub>CH<sub>2</sub>-O-Ar + CH<sub>2</sub>), 4.10 (m, 4H, CH<sub>3</sub>CH<sub>2</sub>-O-Ar), 4.13 (t, 4H, O-CH<sub>2</sub>), 7.36-7.53 (m, 6H, Ar-H), 9.80 (s, 2H, Ar-CHO). <sup>13</sup>C NMR (75 MHz, CDCl<sub>3</sub>,  $\delta$ , ppm): 15.00 (CH<sub>3</sub>), 68.00 (Ar-O-CH<sub>2</sub>), 64.32 (OCH<sub>2</sub>CH<sub>3</sub>) 111.40-152.79 (Ar-C), 191.76 (CHO).

**4,4'-Diformyl- $\alpha,\omega$ -diphenoxy-*p*-xylene (M-2A):** Yield: 88%. M.p.: 157-159 °C. FT-IR (KBr, v, cm<sup>-1</sup>): 2930 (Aliphatic CH), 1688 (CO), 1592 (C=C), 1508 (C=C), 1230 (C-O-C). <sup>1</sup>H NMR (300 MHz, DMSO-*d*<sub>6</sub>,  $\delta$ , ppm): 5.24 (t, 4H, O-CH<sub>2</sub>), 7.20-7.89 (m, 12H, Ar-H), 9.88 (s, 2H, Ar-CHO). <sup>13</sup>C NMR (75 MHz, CDCl<sub>3</sub>,  $\delta$ , ppm): 70.70 (Ar-O-CH<sub>2</sub>-Ar), 129.86-163.46 (Ar-C), 135.00-127.00 (Ar-spacer), 190.69 (CHO).

**4,4'-Diformyl-3,3'-methoxy- $\alpha,\omega$ -diphenoxy-*p*-xylene (M-2B):** Yield: 89%. M.p.: 157-159 °C. FT-IR (KBr, v, cm<sup>-1</sup>): 2933 (Aliphatic CH), 1670 (CO), 1589 (C=C), 1510 (C=C), 1233 (C-O-C). <sup>1</sup>H NMR (300 MHz, DMSO-*d*<sub>6</sub>,  $\delta$ , ppm): 4.12 (s, 6H, CH<sub>3</sub>-O-Ar), 5.25 (s, 4H, O-CH<sub>2</sub>), 7.27-7.60 (m, 10H, Ar-H), 9.83 (s, 2H, Ar-CHO). <sup>13</sup>C NMR (75 MHz, CDCl<sub>3</sub>,  $\delta$ , ppm): 70.19 (Ar-O-CH<sub>2</sub>-Ar), 56.02 (OCH<sub>3</sub>) 110.15-153.73 (Ar-C), 128-136.9 (Ar-spacer), 191.86 (CHO).

**4,4'-Diformyl-3,3'-ethoxy- $\alpha,\omega$ -diphenoxy-*p*-xylene (M-2C):** Yield: 87%. M.p.: 157-159 °C. FT-IR (KBr, v, cm<sup>-1</sup>): 2923 (Aliphatic CH), 1677 (CO), 1581 (C=C), 1521 (C=C), 1223 (C-O-C). <sup>1</sup>H NMR (300 MHz, DMSO-*d*<sub>6</sub>,  $\delta$ , ppm): 1.34 (t.q., 6H, CH<sub>3</sub>CH<sub>2</sub>-O-Ar, <sup>3</sup>J = 6.9 Hz), 4.11 (s, 4H, CH<sub>3</sub>CH<sub>2</sub>-O-Ar, <sup>3</sup>J = 6.9 Hz), 5.25 (s, 4H, O-CH<sub>2</sub>), 7.26-7.52 (m, 10H, Ar-H), 9.82 (s, 2H, Ar-CHO). <sup>13</sup>C NMR (75 MHz, CDCl<sub>3</sub>,  $\delta$ , ppm): 15.00 (OCH<sub>2</sub>CH<sub>3</sub>), 71.13 (Ar-O-CH<sub>2</sub>-Ar), 55.39 (OCH<sub>2</sub>CH<sub>3</sub>), 111.55-154.62 (Ar-C), 129-135.54 (Ar-spacer), 191.88 (CHO).

### 2.3. Biological activities

#### 2.3.1. The free radical (DPPH) scavenging activity

The free radical (DPPH) scavenging activity was performed by using 2,2-diphenyl-1-picrylhydrazyl free radical (DPPH) assay [21-23]. DPPH (3.2 mg) in 100 mL of methanol (82%) were dissolved to prepare 1,10-DPPH solution. The stock solutions of the test bifunctional aldehydes were prepared in DMSO (1 mL) at 1000 ppm concentration level. The stock solutions were further diluted to 100 and 10 ppm. The reaction mixture with a final volume of 3 mL was prepared by adding 2 mL of DPPH solution, 0.9 mL of Tris HCl buffer, and 100  $\mu$ L of the bifunctional aldehyde at 1000, 100 and 10 ppm concentration to obtain the final concentration of 33.33, 3.33, and 0.33 ppm in the reaction. 2 mL of DPPH solution was dissolved in 100  $\mu$ L of DMSO to prepared

negative control. After incubation, sample mixture was kept at room temperature in dark for 30 min. Then, absorbance of the samples was taken at 517 nm on a UV/visible light spectrophotometer next to the blank. Each experiment was repeated thrice time and results were estimated by calculating IC<sub>50</sub> value [16].

### 2.3.2. Antibacterial assay

Antibacterial activity of the bifunctional aldehyde was checked against six bacterial strains viz. including four Gram-negative i.e., *Bordetella bronchioseptica*, *Salmonella typhimurium*, *Escherichia coli*, *Enterobacter aerogenes* and Gram-positive i.e., *Staphylococcus aureus* and *Micrococcus luteus*. Bacterial strains were incubated for 24 h at 1 mg/mL concentration. Roxithomycin, cefixime USP and DMSO were the controls of this test. 100 µL of each samples and controls were transferred in the boreholes of culture plates. Inhibition zones were clearly seen around boreholes of antibiotics and active bifunctional aldehyde with the aid of Vernier caliper subsequently incubation at 37 °C for 24 hours. Bifunctional aldehydes having this activity were then exposed to find least possible inhibitory concentration (MIC). It was examined at minor concentration of active test bifunctional aldehydes (0.8, 0.6, 0.4 and 0.2 mg/mL) [21].

### 2.3.3. Antifungal activities

Antifungal assay was performed to check the activity of the test compounds against five fungal strains viz. *Aspergillus flavus*, *Aspergillus fumigatus*, *Aspergillus niger*, *Fusarium solani* and *Mucor species*. To test the antifungal activity of bifunctional aldehyde, agar tube dilution method was done [24,25]. Sabouraud dextrose agar (6.5 g) (Merck, Darmstadt Germany) was dissolved 100 mL distilled water (pH = 5.6) to culture media. Sabouraud dextrose agar (10 mL) was dispensed in tubes then plugged test tubes and autoclaved at 121 °C for 21 min. Tubes containing the reaction mixture were cool at 50 °C and the Sabouraud dextrose agar was introduced with 67 µL of corresponding test samples dilutions. Then tubes were allowed to solidify in a slanting position at room temperature. Three slants of the test samples were prepared for fungus species. The tubes having solidified media and bifunctional aldehyde were further inoculated with a 4 mm diameter piece of inoculum, taken from seven days old culture of fungus. One test tube of each test sample was prepared for use as positive control. Slants without test samples were used as negative control. The test tubes were incubated at 28 °C for 7 days. Cultures were checked twice weekly during the incubation period. Reading was note down by determining the linear length (mm) of the fungus in slant and growth inhibition was calculated with reference to the negative control. Percentage inhibition of fungal growth for all concentration of the test samples was calculated as:

$$\% \text{ Inhibition of fungal growth} = 100 - \left[ \left\{ \frac{\text{Fungal growth in mm in test sample}}{\text{Fungal growth in mm in control}} \right\} \times 100 \right] \quad (1)$$

### 2.3.4. Brine shrimp lethality assay

Brine shrimp lethality assay was used to assess the cytotoxicity of the compounds [26,27]. Artificial sea water (pH = 7.4) was prepared by dissolving commercial sea salt (34 g/mL) in distilled water. Brine shrimp eggs were allowed to hatch in the artificial sea water for 48 hours under bright light at 37 °C. After 48 hours, the hatched shrimp napulii were collected using a Pasteur pipette. Fifteen shrimps were transferred to each vial containing 5 mL of artificial sea water and 200, 66.6, 22.2, 7.4 and 2.5 µg/mL final concentration of

each test compound from their stock solutions. The vials were incubated at room temperature under direct illumination. After 24 hours, the number of live shrimps present in each vial was counted. The assay was performed in triplicate. The data was analyzed by probity analysis using Finney software to determine the LD<sub>50</sub> (Lethal Dose that killed 50% of shrimps) values.

### 2.3.5. Potato disc antitumor assay

Potato disc antitumor assay was performed to assess the antitumor activity of the test compounds [27,28]. The assay was performed in aseptic conditions. Potato cylinders were cut out from healthy surface-sterilized potatoes using cork borers (8 mm bore diameter). The cylinders were cut into 5 mm thick discs. Ten disks were placed on solidified supporting medium (1.5% agar solution in distilled water) in each petri plate. For each test compound to be assayed, four different inoculums, corresponding to four different concentrations, were prepared. To prepare inocula, 750 µL of distilled water and 600 µL of broth culture of *Agrobacterium tumefaciens* (At-10, 48 hours growth) were added to 150 µL of the serially diluted stock solutions such that the final concentrations of the test compound in the inocula were 200, 66.6, 22.2 and 7.4 µg/mL, respectively. To the surface of each potato disc, 50 µL of inoculum of respective concentrations of test compound as well as controls was added. Inoculum was allowed to diffuse into the discs for 10 min and the plates were then sealed with parafilm. These plates were incubated at 28 °C for 21 days. The assay was carried out in triplicate and number of tumors on each disc was counted after staining the discs with Lugol's reagent (5% I<sub>2</sub> and 10% KI solution in distilled water). Percentage inhibition was calculated using formula:

$$\% \text{ Tumor inhibition} = 100 - \left[ \left\{ \frac{\text{Number of tumor in test sample}}{\text{Number of tumors in control}} \right\} \times 100 \right] \quad (2)$$

### 2.3.6. DNA damaging assay

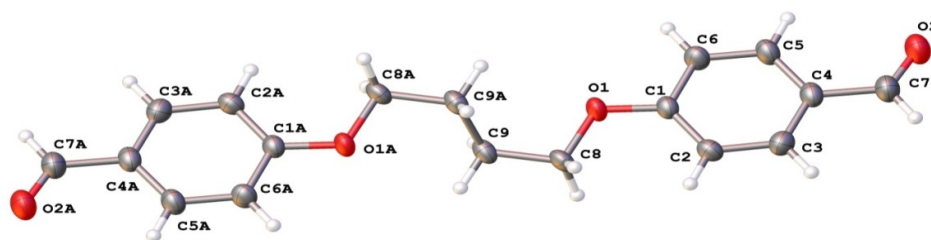
The effect of bifunctional aldehyde on plasmid DNA in vitro was carried out by the described literature method [21-23]. The reaction was performed in Eppendorf tube at a final volume of 15 µL having the following components, 0.5 µg pBR322 DNA suspended in 3 µL of 50 mM phosphate buffer (pH = 7.4), 3 µL of 2 mM FeSO<sub>4</sub>, 5 µL of tested bifunctional aldehyde samples and 4 µL of 30% of H<sub>2</sub>O<sub>2</sub>. Treatment of pBR322DNA with FeSO<sub>4</sub> and H<sub>2</sub>O<sub>2</sub> was used as a positive control. Then, final mixture was incubated at 37 °C for 1 h at 100 V. DNA bands (super coiled, linear and open circular) were strained with ethidium bromide were examined qualitatively by scanning with Doc-IT computer program (VWR). Antioxidant or prooxidant effects on DNA were analyzed on rise or damage percentage of supercoiled samples, paralleled with control value. Experiment was done in the dark to elude the effect of photo-oxidation of samples [21].

### 2.4. XRD structural analysis

The data for M1-A and M1-C were collected at 150 K on a Bruker Apex II CCD diffractometer using MoK<sub>α</sub> radiation (λ = 0.71073 Å). The data for M2-A were collected at 173 K on a Stoe IPDS II diffractometer using MoK<sub>α</sub> radiation (λ = 0.71073 Å). The structures were solved by direct methods [29] and refined on F<sup>2</sup> using all the reflections [30]. All the non-hydrogen atoms were refined using anisotropic atomic displacement parameters and hydrogen atoms were inserted at calculated positions using a riding model. Parameters for data collection and refinement are summarized in the Table 1.

**Table 1.** Crystal data and structure refinement for M-1A, M-1C and M-2A.

Crystal parameters	M-1A	M-1C	M-2A
Empirical formula	C <sub>18</sub> H <sub>18</sub> O <sub>4</sub>	C <sub>22</sub> H <sub>22</sub> O <sub>6</sub>	C <sub>22</sub> H <sub>18</sub> O <sub>4</sub>
Formula weight	298.32	386.43	346.36
Temperature (K)	150(2)	150(2)	173(2)
Crystal system	Triclinic	Monoclinic	Monoclinic
Space group	P-1	P2 <sub>1</sub> /n	P2 <sub>1</sub> /n
a (Å)	4.4952(10)	4.8246(4)	10.0170(14)
b (Å)	7.9550(18)	8.4869(7)	9.5713(9)
c (Å)	11.067(3)	25.100(2)	18.216(2)
α (°)	73.849(3)	90.00	90.00
β (°)	84.705(3)	94.4540(10)	94.761(11)
γ (°)	80.851(3)	90.00	90.00
Volume (Å <sup>3</sup> )	374.81(15)	1024.65(15)	1740.4(3)
Z	1	2	4
ρ <sub>calc</sub> (g/cm <sup>3</sup> )	1.322	1.252	1.322
μ (mm <sup>-1</sup> )	0.093	0.091	0.091
F(000)	158.0	412.0	728.0
Crystal size (mm <sup>3</sup> )	0.26 × 0.21 × 0.01	0.24 × 0.22 × 0.11	0.48 × 0.47 × 0.47
Radiation	MoKα (λ = 0.71073)	MoKα (λ = 0.71073)	MoKα (λ = 0.71073)
θ range for data collection (°)	3.84 to 50	5.06 to 54	7.2 to 51.4
Index ranges	-5 ≤ h ≤ 5, -9 ≤ k ≤ 9, -13 ≤ l ≤ 13	-6 ≤ h ≤ 6, -10 ≤ k ≤ 10, -31 ≤ l ≤ 31	-12 ≤ h ≤ 9, -11 ≤ k ≤ 11, -22 ≤ l ≤ 22
Reflections collected	2975	9222	8688
Independent reflections	1316 [R <sub>int</sub> = 0.0312]	2236 [R <sub>int</sub> = 0.0286]	3236 [R <sub>int</sub> = 0.0394]
Data/restraints/parameters	1316/0/100	2236/0/127	3236/0/236
Goodness-of-fit on F <sup>2</sup>	1.023	1.035	1.035
Final R indexes [I ≥ 2σ (I)]	R <sub>1</sub> = 0.0508, wR <sub>2</sub> = 0.1179	R <sub>1</sub> = 0.0383, wR <sub>2</sub> = 0.0939	R <sub>1</sub> = 0.0376, wR <sub>2</sub> = 0.1004
Final R indexes [all data]	R <sub>1</sub> = 0.0941, wR <sub>2</sub> = 0.1390	R <sub>1</sub> = 0.0496, wR <sub>2</sub> = 0.1003	R <sub>1</sub> = 0.0489, wR <sub>2</sub> = 0.1053
Largest diff. peak/hole (e.Å <sup>-3</sup> )	0.30/-0.19	0.25/-0.17	0.19/-0.16
CCDC	960622	960623	1498777

**Figure 2.** Molecular structure of 4,4'-diformyl- $\alpha,\omega$ -diphenoxybutane (M-1A). Non-hydrogen atoms are shown as 50% probability ellipsoids and hydrogen atoms as spheres of arbitrary radius. The suffix "A" indicates an atom generated under symmetry operation  $A = -x+1, -y+1, -z+1$ .

### 3. Results and discussion

Aliphatic (4,4'-diformyl- $\alpha,\omega$ -diphenoxybutane (M-1A), 4,4'-diformyl-3,3'-methoxy- $\alpha,\omega$ -diphenoxybutane (M-1B) and 4,4'-diformyl-3,3'-ethoxy- $\alpha,\omega$ -diphenoxybutane (M-1C)) and aromatic (4,4'-diformyl- $\alpha,\omega$ -diphenoxy-*p*-xylene (M-2A), 4,4'-diformyl-3,3'-methoxy- $\alpha,\omega$ -diphenoxy-*p*-xylene (M-2B), 4,4'-diformyl-3,3'-ethoxy- $\alpha,\omega$ -diphenoxy-*p*-xylene (M-2C)) spacer containing bifunctional aldehyde compounds were synthesized (Figure 1) [19,20] and structurally analyzed. In this study, various biological assays were also discussed in detail. The results of each study are discussed under separate headings below.

#### 3.1. XRD structural analysis

The structure of M-1A, M-2A and M-1C was determined in a single crystal X-ray diffraction study. Figure 2-4 show the labelled structure and Figure 5 shows hydrogen bonds of M-1A. Details of crystal structure determination are summarized in Table 1, and the bond lengths, bond angles and the calculated values for hydrogen-bond geometry are given in supplementary information. In M-1A, there are weak C-H...O hydrogen bonds linking the molecules into sheets parallel to the (102) plane, but there are no significant interactions between the sheets and this probably accounts for the crystal habit (thin sheets). There are no corresponding interactions in M-1C and M-2A, where the packing is likely to be controlled by van der Waals interactions between the alkyl chains and the aromatic rings.

#### 3.2. Biological evaluations

In this study, numerous biological assays were performed on the series of bifunctional aldehyde to identify potential therapeutic agents having cytotoxic, antifungal, antibacterial, antioxidant, antitumor and DNA-interaction and damaging activities. The results of each assay are discussed under separate headings below.

##### 3.2.1. Antibacterial assay

The compounds were tested for their antibacterial activity against six different strains viz. *S. aureus*, *S. typhimurim*, *E. coli*, *E. aerogenes*, *M. luteus*, and *B. bronchioseptica*. Bifunctional aldehyde which tested positive in initial screening (Disc diffusion method) were further tested on microtitre plate to determine their MIC values. In comparison, aromatic spacer containing bifunctional aldehyde (M-2A and M-2C) showed good antibacterial activity as compared to the aliphatic spacer containing bifunctional aldehyde [31]; however their activity was very selective. M-2A was active against *E. coli*, *E. aerogenes* and *M. luteus*; while M-2C showed antibacterial activity against *E. coli* (Figure 6 of representative dialdehyde M-2A) and *M. luteus* only. The results are summarized in Table 2.

##### 3.2.2. DPPH free radical scavenging assay

The antioxidant activity of the compounds was tested (at four different concentrations) by spectrophotometrically assessing their ability to scavenge free radicals.



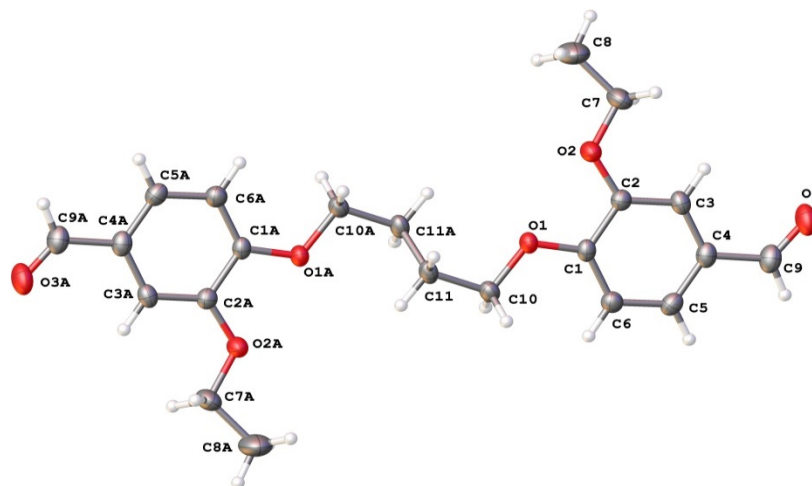


**Figure 3.** Molecular structure of 4,4'-diformyl-3,3'-ethoxy- $\alpha,\omega$ -diphenoxybutane (M-1C). Non-hydrogen atoms are shown as 50% probability ellipsoids and the suffix "A" indicates an atom generated under symmetry operation  $-x+2, -y+1, -z+1$ .

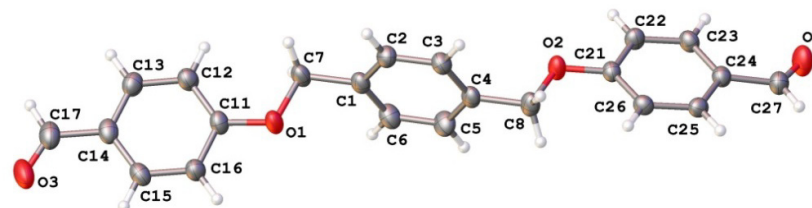


**Figure 4.** Molecular structure of 4,4'-diformyl- $\alpha,\omega$ -diphenoxy-*p*-xylene (M-2A). All the non-hydrogen atoms were refined using anisotropic atomic displacement parameters and hydrogen atoms were inserted at calculated positions using a riding model.

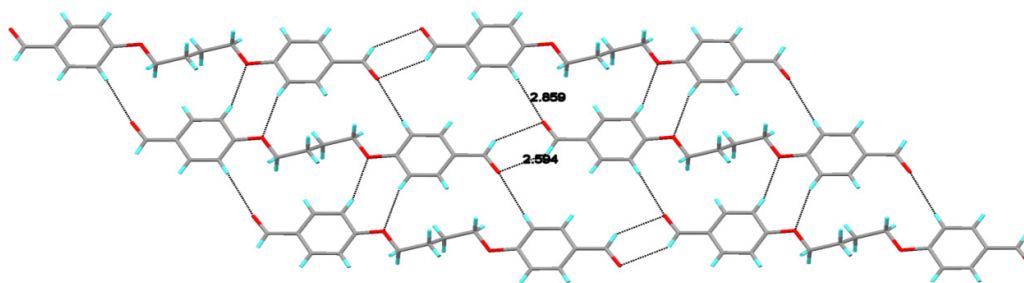


**Figure 5.** Hydrogen bonded sheets of 4,4'-diformyl- $\alpha,\omega$ -diphenoxybutane (M-1A).

None of the bifunctional aldehyde showed any antioxidant potential except M-2A compound (aromatic spacer) (Figure 7). The  $IC_{50}$  value of M-2A was 55 ppm. The results are summarized in Table 3.

### 3.2.3. Antifungal assay

The compounds were tested for their antifungal activity against five different strains viz. *A. niger*, *A. fumigatus*, *A. flavus*, *Mucor sp.*, and *F. solani*. The growth inhibition for representative M-2A bifunctional aldehyde is presented at different 200, 100, 50 and 25 ppm level in Figure 8. Overall, the compounds did not show significant antifungal activity. Aliphatic spacer containing bifunctional aldehyde (M-1A, M-1B) failed to show antifungal activity against any of the strains except M-1C. Only aromatic containing bifunctional aldehyde (M-2A, M-2C) showed significant antifungal activity. M-1C and M-2C was active against *A. fumigatus* and *Mucor sp.* only;

whereas M-2A showed antifungal activity against *F. solani* and *A. fumigatus* only. Both categories of bifunctional aldehyde were inactive against *A. niger* and *A. flavus*. The results are summarized in Table 4.

### 3.2.4. Cytotoxicity assay

Cytotoxicity of synthesized compounds was determined by investigating their *in vivo* lethality to shrimp larvae.  $LD_{50}$  values were calculated using the Finney software. Bifunctional aldehyde was found to be highly cytotoxic. Amongst the synthesized compounds, phenyl ring containing bifunctional aldehyde M-2A showed the best cytotoxic activity as compared to the aliphatic spacer compounds. Methoxy and ethoxy substituted aromatic bifunctional aldehyde (M-2B and M-2C) showed low  $LD_{50}$  values indicating their significant cytotoxic potential as compared to substituted aliphatic bifunctional aldehyde. The cytotoxic results are summarized in Table 5.

**Table 2.** Results of antibacterial assay.

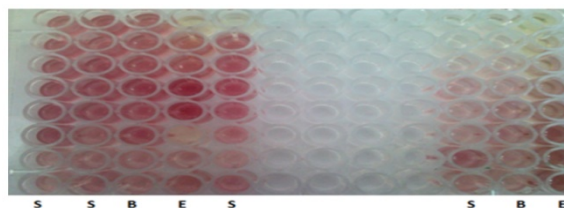
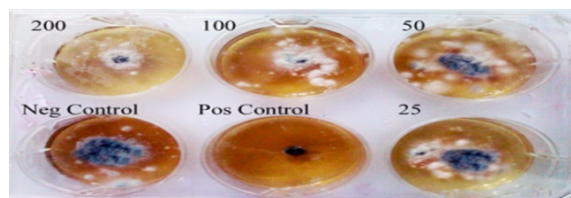
Sample	% zone of inhibition of samples (mm)					
	<i>S. aureus</i>	<i>S. typhimurium</i>	<i>E. coli</i>	<i>E. aerogenes</i>	<i>M. luteus</i>	<i>B. bronchioseptica</i>
M-1A	0	0	0	0	0	0
M-1B	0	0	0	0	0	0
M-1C	0	0	0	0	0	0
M-2A	0	0	25	25	12.5	0
M-2B	0	0	0	0	0	0
M-2C	0	0	25	0	50	0
Cefixime	24.2	30.4	32.2	27.8	21.6	32.3

**Table 3.** Results of DPPH free radical scavenging assay.

Sample	Percentage scavenging at concentrations					IC <sub>50</sub> value (ppm)
	200 ppm	66.6 ppm	22.2 ppm	7.4 ppm	2.5 ppm	
M-1A	0	0	0	0	0	0
M-1B	4.7	1.5	0	3.2	-1.58	>200
M-1C	0	0	0	0	0	0
M-2A	0	61.1	17.5	16.6	-1.58	55
M-2B	0	19.8	11.1	10.3	8.7	>200
M-2C	0	-1.58	-7	-9.5	-4.7	>200

**Table 4.** Results of antifungal assay.

Sample	<i>A. fumigatus</i>				<i>Mucor sp.</i>				<i>F. solani</i>			
	Percentage inhibition at conc. (ppm)				Percentage inhibition at conc. (ppm)				Percentage inhibition at conc. (ppm)			
	200	100	50	25	200	100	50	25	200	100	50	25
M-1A	0	0	0	0	0	0	0	0	0	0	0	0
M-1B	0	0	0	0	0	0	0	0	0	0	0	0
M-1C	12	6	0	0	25	20	10	10	0	0	0	0
M-2A	33	27	20	0	0	0	0	0	47	22	0	0
M-2B	0	0	0	0	0	0	0	0	0	0	0	0
M-2C	63	17	6	0	55	39	21	5	0	0	0	0
Terbinafine	100				100				100			

**Figure 6.** Antibacterial activity of M-2A against S = *S. aureus*, E = *E. coli* and B = *B. bronchioseptica*.**Figure 7.** DPPH free radical scavenging activity of compound M-2A at 5 different concentrations labeled as a = 200 ppm, b = 66.6 ppm, c = 22.2 ppm, d = 7.4 ppm and e = 2.5 ppm. Whereas PC = Positive control and NC = Negative control.**Figure 8.** Growth inhibition of *Fusarium solani* at four different concentrations (200, 100, 50 and 25 ppm) of M-2A. Pos Control = Positive control, Neg Control = Negative control.

The results of the cytotoxicity assay are in accordance with previous reports in the literature. The cytotoxicity of compounds containing aldehyde groups has been reported earlier [32,33].

### 3.2.5. Tumor inhibition

As the bifunctional aldehyde showed significant cytotoxic activity therefore they were tested for their tumor inhibition

potential. Potato disk tumor induction is prompt, inexpensive, simple trustworthy test for sensing antitumor agents. This assay was based on *A. tumefaciens* infection and as the mechanisms is quite alike in plants and animals therefore it reveal a good correlation in results as compare to the other most normally used antitumor screening assays. The compounds were tested for their potential antitumor activity using the potato disc antitumor assay; and the results are mentioned in Table 5.

**Table 5.** Results of cytotoxic assay \*.

Sample	Total no. of shrimps	No. of shrimps killed at dose level					LD <sub>50</sub> value (ppm)
		200 ppm	66.6 ppm	22.2 ppm	7.4 ppm	2.5 ppm	
M-1A	30	10	7	7	6	2	>200
M-1B	30	29	26	17	11	9	10.48
M-1C	30	28	26	22	18	16	2.56
M-2A	30	29	28	26	25	24	0.06
M-2B	30	28	26	22	18	16	2.58
M-2C	30	30	22	19	11	08	11.54

\* LD<sub>50</sub>= Lethality dose.**Table 6.** Results of tumor inhibition assay.

Sample	Percentage inhibition±SD *				IC <sub>50</sub> value (ppm)
	200 ppm	66.6 ppm	22.2 ppm	7.4 ppm	
M-1A	90.00±1.4	88.75±1.6	70.00±0.6	61.25±2.2	0.73
M-1B	95.00±0.5	91.25±1.8	92.50±1.5	62.50±1.3	7.66
M-1C	36.25±1.3	36.88±4.0	19.38±1.2	8.29±1.1	>200
M-2A	71.25±1.5	46.25±2.0	40.00±1.1	16.25±2.0	58.07
M-2B	40.00±0.5	35.00±1.6	27.62±3.0	18.75±2.1	>200
M-2C	58.75±1.2	57.50±1.8	58.75±0.5	47.50±3.3	10.67

\* SD = Standard deviation.

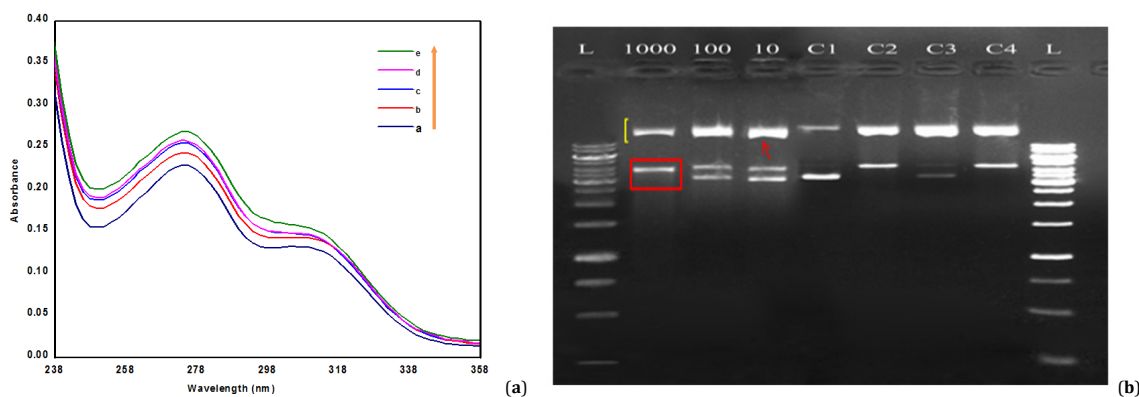


**Figure 9.** a) UV/Vis signature of the interaction between free M-1A and DNA in Melvaine buffer solution  $C_{M-1A} = 5.0 \mu\text{M}$ . From a to e:  $C_{DNA} = 0, 20, 40, 60$  and  $100 \mu\text{M}$  (pH = 7.4, T = 309.5 K). b) Agarose gel electrophoresis pattern of pBR322 DNA exposed to M-1A at various concentrations: L, DNA Ladder (kb); 1000 ppm, plasmid + 1000 ppm of M-1A +  $\text{FeSO}_4 + \text{H}_2\text{O}_2$  with no lower band; 100 ppm, plasmid + 100 ppm of M-1A +  $\text{FeSO}_4 + \text{H}_2\text{O}_2$  weak lower band thickness; 10 ppm, plasmid + 10 ppm of M-1A +  $\text{FeSO}_4 + \text{H}_2\text{O}_2$  with slightly decrease band thickness; C1, 3  $\mu\text{L}$  of diluted plasmid DNA and 12  $\mu\text{L}$  of phosphate buffer; C2, 3  $\mu\text{L}$  diluted plasmid, 3  $\mu\text{L}$   $\text{FeSO}_4$  and 9  $\mu\text{L}$  phosphate buffer; C3, 3  $\mu\text{L}$  diluted plasmid, 4  $\mu\text{L}$   $\text{H}_2\text{O}_2$  and 8  $\mu\text{L}$  phosphate buffer; C4, 3  $\mu\text{L}$  diluted plasmid, 4  $\mu\text{L}$   $\text{H}_2\text{O}_2$ , 3  $\mu\text{L}$   $\text{FeSO}_4$  and 5  $\mu\text{L}$  of phosphate buffer.

All the synthesized bifunctional aldehyde show antitumor activity. In comparison of aryl and alkyl linker based bifunctional aldehyde; best antitumor activity was shown by M-1A with tumor inhibition IC<sub>50</sub> value 0.73 ppm than the corresponding bifunctional aldehyde M-1B and M-1C. The test compounds successfully inhibited *Agrobacterium tumefaciens* mediated tumor formation on potato discs [20,34]. Effect of concentration remained significant at  $p < 0.05$  (Table 6) in ANOVA by the MSTATC software.

### 3.3. DNA-Drug interaction assay

One of the primary steps in the discovery of anti-cancerous drugs is to evaluate their DNA-binding/interaction ability. As anticancer therapies often target the DNA of the cancerous cells, thus DNA-drug interaction assay becomes imperative for designing of new anti-cancerous drugs [35].

#### 3.3.1. Electronic absorption spectroscopy of bifunctional aldehyde

The interaction of bifunctional aldehyde with DNA was further investigated with the help of UV-vis spectroscopy. Aliphatic based bifunctional aldehyde show only one absorbance band in the range of 290-297 nm while aromatic linker containing bifunctional aldehyde show two absorbance bands because of aromatic ring in between the bifunctional aldehyde. These absorptions in aromatic based bifunctional

aldehyde may be attributed to the  $\pi-\pi^*$  and  $n-\pi^*$  transitions. Drug interaction assay was performed on the entire bifunctional aldehyde. After addition of DNA, there is an increase in the absorbance (hyperchromism) which might be due to non-intercalative and damaging behavior with DNA. The aromatic  $n-\pi^*$  and  $\pi-\pi^*$  states of the planar group seem to interact strongly with the electronic states of the DNA bases causing an extensive hyperchromic effect with no significant shift in peak [36,37]. Wavelength (nm) values of all the bifunctional aldehydes are presented in Table 7. DNA-bifunctional aldehyde interaction signature of representative dialdehyde M-2A is shown in Figure 9a shows two peaks in the lower wavelength region (at 270 and 315 nm).

#### 3.3.2. DNA damaging assay

DNA damaging activity was performed in vitro at 10, 100 and 1000 ppm concentration of bifunctional aldehyde (Figure 9b). With the attack of OH radical, super coiled DNA (pBR322 DNA) was distorted into open circular. Effect of bifunctional aldehyde at different concentration i.e 1000, 100 and 10 ppm on the plasmid DNA were studied in the presence of positive control (pBR322DNA with  $\text{FeSO}_4$  and  $\text{H}_2\text{O}_2$ ) [21-23]. The results of the assay for bifunctional aldehyde have as is obvious in Table 4 that only 1000 ppm has not shown any DNA protection potential (no lower band observed) whereas rest of the concentrations 100 and 10 ppm has shown plasmid protection potential but with weak damaging effects.

**Table 7.** UV-Visible spectroscopy and DNA damaging studies of bifunctional aldehyde \*.

Sample	DNA damaging assay			Wavelength (nm)
	1000 ppm	100 ppm	10 ppm	
M-1A	+++	+-	-	290
M-1B	+++	+-	-	292
M-1C	+++	+-	-	297
M-2A	+++	++	+	270, 315
M-2B	+++	++	+	282, 313
M-2C	+++	++	+	290, 305

\* +++ = v. strong; ++ = medium; + = small; - = v. slight.

By increasing the concentrations, thickness of the each upper band have reduced. Among bifunctional aldehyde compounds; best DNA damaging activity were shown by aromatic linkers than the aliphatic containing bifunctional aldehyde. All the results are summarized in Table 7.

#### 4. Conclusions

Bifunctional aldehyde has tremendous efficacy and broad biological spectrum of activities i.e antibacterial, antifungal, antioxidant, antitumor and cytotoxic. On the basis of structure activity relationship, aromatic linker containing bifunctional aldehyde show good pharmacological activities as compared to the aliphatic based bifunctional aldehyde. Hyperchromic effect in UV-vis spectroscopy is suggestive of bifunctional aldehyde-DNA interaction which could lead to DNA damage also. It is further complemented by results obtained from DNA damaging assay. On the basis of their potential antitumor activity, bifunctional aldehyde moiety can be attributed to have the potential to be developed as chemo-therapeutic agents.

#### Supplementary material

CCDC-960622 (M-1A), 960623 (M-1C) and 1498777 (M-2A) contain the supplementary crystallographic data for this paper. The data can be obtained free of charge at <http://www.ccdc.cam.ac.uk/const/retrieving.html> or from the Cambridge Crystallographic Data Centre (CCDC), 12 Union Road, Cambridge CB2 1EZ, UK; fax: +44(0)1223-336033 or e-mail: [deposit@ccdc.cam.ac.uk](mailto:deposit@ccdc.cam.ac.uk).

#### References

- Wang, Q.; Bao, L.; Jia, C.; Li, M.; Li, J. J.; Lu, X. *BMC Biotechnol.* **2017**, *17*(1), 31, pp. 1-9.
- Ebada, M. E. J. *Pharmacol. Clin. Res.* **2017**, *2*(2), 555585, pp. 1-4.
- Sterner, O.; Carter, R. E.; Nilsson, L. M. *Mut. Res. Genetic Toxicol.* **1987**, *188*(3), 169-174.
- Cimino, G.; De Rosa, S.; De Stefano, S.; Sodano, G.; Villani, G. *Science* **1983**, *219*(4589), 1237-1238.
- Rashidi, M. R.; Soltani, S. *Exp. Opin. Drug Discov.* **2017**, *12*(3), 305-316.
- Abe, M.; Ozawa, Y.; Uda, Y.; Yamada, F.; Morimitsu, Y.; Nakamura, Y.; Osawa, T. *Biosci., Biotech. Biochem.* **2004**, *68*(7), 1601-1604.
- Fraud, S.; Maillard, J. Y.; Russell, A. D. J. *Hosp. Inf.* **2001**, *48*(3), 214-221.
- Kubo, I.; Himejima, M. *Experientia* **1992**, *48*(11-12), 1162-1164.
- Anke, H.; Sterner, O. *Planta Medica* **1991**, *57*(4), 344-346.
- Hobro, A. J.; Smith, N. I. *Vib. Spectrosc.* **2017**, *91*, 31-45.
- Dvonch, W.; Fletcher, H.; Gregory, F. J.; Healy, E. M. H.; Warren, G. H.; Alburn, H. E. *Cancer Res.* **1966**, *26*(11), 2386-2389.
- Giraldi, T.; Goddard, P. M.; Nisi, C.; Sigon, F. J. *Pharm. Sci.* **1980**, *69*(1), 97-98.
- Billman, J. H.; Tonnis, J. A. J. *Pharm. Sci.* **1971**, *60*(8), 1188-1192.
- Minotti, G.; Menna, P.; Salvatorelli, E.; Cairo, G.; Gianni, L. *Pharmacolog. Rev.* **2004**, *56*(2), 185-229.
- Jacobs, A. T.; Marnett, L. J. *Acc. Chem. Res.* **2010**, *43*(5), 673-683.
- Nadkarni, D. V.; Sayre, L. M. *Chem. Res. Toxicol.* **1995**, *8*(2), 284-291.
- Brooks, P. J.; Theruvathu, J. A. *Alcohol* **2005**, *35*(3), 187-193.
- Voulgaridou, G. P.; Anastopoulos, I.; Franco, R.; Panayiotidis, M. I.; Pappa, A. *Mut. Res. / Fundam. Mol. Mechan. Mutagen.* **2011**, *711*(1), 13-27.
- Li, C. H.; Chang, T. C. J. *Polymer Sci. A: Polymer Chem.* **1991**, *29*(3), 361-367.
- Kaya, I.; Koyuncu, S.; Culhaoglu, S. *Polymer* **2008**, *49*(3), 703-714.
- Gul, A.; Akhter, Z.; Siddiq, M.; Sarfraz, S.; Mirza, B. *Macromolecules* **2013**, *46*(7), 2800-2807.
- Nawaz, H.; Akhter, Z.; Yameen, S.; Siddiqi, H. M.; Mirza, B.; Rifat, A. J. *Organometal. Chem.* **2009**, *694*(14), 2198-2203.
- Sultan, M. T.; Butt, M. S.; Anjum, F. M.; Jamil, A.; Akhtar, S.; Nasir, M. *Pak. J. Bot.* **2009**, *41*(3), 1321-1330.
- Oliveira-Brett, A. M.; Piedade, J. A. P.; Silva, L. A.; Diculescu, V. C. *Anal. Biochem.* **2004**, *332*(2), 321-329.
- Oliveira-Brett, A. M.; Diculescu, V.; Piedade, J. A. P. *Bioelectrochem.* **2002**, *55*(1), 61-62.
- McLaughlin, J. L.; Rogers, L. L.; Anderson, J. E. *Drug Infor. J.* **1998**, *32*(2), 513-524.
- Shabbir, M.; Akhter, Z.; Ashraf, A. R.; Bolte, M.; Wahid, S.; Mirza, B. *Eur. J. Chem.* **2017**, *8*(1), 46-51.
- Ahmad, M. S.; Hussain, M.; Hanif, M.; Ali, S.; Qayyum, M.; Mirza, B. *Chem. Biol. Drug Design* **2008**, *71*(6), 568-576.
- Sheldrick, G. M. *Acta Cryst. A* **2008**, *64*, 112-122.
- Sheldrick, G. M. *Acta Cryst. C* **2015**, *71*, 3-8.
- Gilles, M.; Zhao, J.; An, M.; Agboola S. *Food Chem.* **2010**, *119*, 731-737.
- Anke, H.; Sterner, O. *Planta Medica* **1991**, *57*(4), 344-346.
- Allouche, N.; Apel, C.; Martin, M. T.; Dumontet, V.; Gueritte, F.; Litaudon, M. *Phytochem.* **2009**, *70*(4), 546-553.
- Lunde, C. S.; Kubo, I. *Antimicrob. Agent. Chemother.* **2000**, *44*(7), 1943-1953.
- Ryu, D. D.; Nam, D. H. *Biotechn. Progr.* **2000**, *16*(1), 2-16.
- Oliveira-Brett, A. M.; Diculescu, V.; Piedade, J. A. P. *Bioelectrochem.* **2002**, *55*(1), 61-62.
- Li, Q.; Yang, P.; Wang, H.; Guo, M. J. *Inorg. Biochem.* **1996**, *64*(3), 181-195.